Dynamic phase imaging of microscopic measurements using parallel interferograms generated from a cyclic shear interferometer

Noel-Ivan Toto-Arellano,[1,*] Victor H. Flores-Muñoz,[2] and Belen Lopez-Ortiz[1]

[1] *Centro de Tecnologías Ópticas y Fotónicas, Universidad Tecnológica de Tulancingo, Tulancingo, Hgo., Mexico*
[2]*Centro de Investigaciones en Óptica A.C., León, Gto., Mexico*
[*]*noel.toto@utec-tgo.edu.mx*

Abstract: We present a technique which allows us to generate two parallel interferograms with phase shifts of π/2 using a Cyclic Shear Interferometer (CSI) and a polarizing splitter. Because of the use of a CSI, we obtain the derivative phase data map directly, due to its configuration, it is immune to vibrations because the reference wavefront and the object wavefront have a common path; the shearing interferometer is insensitive to temperature and vibration. To obtain the optical phase data map, two interferograms are generated by collocating a polarizing device at the output of the CSI. The optical phase was processed using a Vargas-Quiroga algorithm. Related experimental results obtained for dynamic microscopic transparent samples are presented.

OCIS codes: (110.0180) Microscopy; (120.3180) Interferometry; (120.5050) Phase measurement; (170.1530) Cell analysis; (170.3880) Medical and biological imaging.

References and links

1. N.-I. Toto-Arellano, D. I. Serrano-García, A. Martínez-García, G. Rodríguez Zurita, and A. Montes-Pérez, "4D profile of phase objects through the use of a simultaneous phase shifting quasi-common path interferometer," J. Opt. **13**(11), 115502 (2011).
2. J. E. Millerd, N. Brock, J. Hayes, M. North-Morris, M. Novak, and J. Wyant, "Pixelated phase-mask dynamic interferometer," Proc. SPIE **5531**, 304–314 (2004).
3. M. N. Morris, J. Millerd, N. Brock, J. Hayes, and B. Saif, "Dynamic phase-shifting electronic speckle pattern interferometer," Proc. SPIE **5869**, 58691B (2005).
4. J. E. Millerd and J. C. Wyant, "Simultaneous phase-shifting Fizeau interferometer," U.S. Patent 7,057,738 B2 (2006).
5. B. Barrientos García, A. J. Moore, C. Pérez-López, L. Wang, and T. Tschudi, "Transient deformation measurement with electronic speckle pattern interferometry by use of a holographic optical element for spatial phase stepping," Appl. Opt. **38**(28), 5944–5947 (1999).
6. B. Barrientos-García, A. J. Moore, C. Pérez-López, L. Wang, and T. Tschudi, "Spatial phase-stepped interferometry using a holographic optical element," Opt. Eng. **38**(12), 2069–2074 (1999).
7. J. C. Wyant, "Dynamic interferometry," Opt. Photon. News **14**(4), 36–41 (2003).
8. T. Kiire, S. Nakadate, and M. Shibuya, "Simultaneous formation of four fringes by using a polarization quadrature phase-shifting interferometer with wave plates and a diffraction grating," Appl. Opt. **47**(26), 4787–4792 (2008).
9. N. I. Toto-Arellano, G. Rodriguez-Zurita, C. Meneses-Fabian, and J. F. Vázquez-Castillo, "A single-shot phase-shifting radial-shearing interferometer," J. Opt. A, Pure Appl. Opt. **11**(4), 045704 (2009).
10. P. Gao, B. Yao, J. Min, R. Guo, J. Zheng, T. Ye, I. Harder, V. Nercissian, and K. Mantel, "Parallel two-step phase-shifting point-diffraction interferometry for microscopy based on a pair of cube beamsplitters," Opt. Express **19**(3), 1930–1935 (2011).
11. Y. Zhu, J. Chen, H. Liu, R. Zhu, and Y. Xiao, "Nonlinear calibrating for phase-shifting adapter with three PZTs," Microw. Opt. Technol. Lett. **23**(4), 209–212 (1999).
12. C. Ai and J. C. Wyant, "Effect of piezoelectric transducer nonlinearity on phase shift interferometry," Appl. Opt. **26**(6), 1112–1116 (1987).
13. Y.-Y. Cheng and J. C. Wyant, "Phase shifter calibration in phase-shifting interferometry," Appl. Opt. **24**(18), 3049–3052 (1985).
14. O. E. Nyakang, G. K. Rurimo, and P. M. Karimi, "Optical phase shift measurements in interferometry," Int. J. Optoelectron. Eng. **3**(2), 13–18 (2013).

#212965 - $15.00 USD Received 30 May 2014; revised 28 Jul 2014; accepted 29 Jul 2014; published 13 Aug 2014

15. J. Vargas, J. A. Quiroga, C. O. S. Sorzano, J. C. Estrada, and J. M. Carazo, "Two-step interferometry by a regularized optical flow algorithm," Opt. Lett. **36**(17), 3485–3487 (2011).
16. J. Quiroga and M. Servin, "Isotropic n-dimensional fringe pattern normalization," Opt. Commun. **224**(4–6), 221–227 (2003).
17. J. Min, B. Yao, P. Gao, R. Guo, J. Zheng, and T. Ye, "Parallel phase-shifting interferometry based on Michelson-like architecture," Appl. Opt. **49**(34), 6612–6616 (2010).
18. A.-H. Phan, M. L. Piao, J.-H. Park, and N. Kim, "Error analysis in parallel two-step phase-shifting method," Appl. Opt. **52**(11), 2385–2393 (2013).
19. X. F. Meng, L. Z. Cai, X. F. Xu, X. L. Yang, X. X. Shen, G. Y. Dong, and Y. R. Wang, "Two-step phase-shifting interferometry and its application in image encryption," Opt. Lett. **31**(10), 1414–1416 (2006).
20. P. Rastogi, ed., *Digital Speckle Pattern Interferometry and Related Techniques* (John Wiley, 2001).
21. W. Steinchen and L. X. Yang, *Digital Shearography; Theory and Application of Digital Speckle Pattern Shearing Interferometry* (SPIE Press, 2003).
22. T. W. Ng, "Digital speckle pattern interferometer for combined measurements of out-of-plane displacement and slope," Opt. Commun. **116**(1–3), 31–35 (1995).
23. B. Bhaduri, N. K. Mohan, and M. P. Kothiyal, "A dual-function ESPI system for the measurement of out-of-plane displacement and slope," Opt. Lasers Eng. **44**(6), 637–644 (2006).
24. N.-I. Toto-Arellano, A. Martínez-García, G. Rodríguez-Zurita, J. A. Rayas-Álvarez, and A. Montes-Perez, "Slope measurement of a phase object using a polarizing phase-shifting high-frequency Ronchi grating interferometer," Appl. Opt. **49**(33), 6402–6408 (2010).
25. J. Márquez-Luna, "Técnicas de colecta y preservación de insectos," Bol. Soc. Entomol. Aragonesa **37**, 385–408 (2005).
26. I. Shock, A. Barbul, P. Girshovitz, U. Nevo, R. Korenstein, and N. T. Shaked, "Optical phase nanoscopy in red blood cells using low-coherence spectroscopy," J. Biomed. Opt. **17**(10), 101509 (2012).
27. H. Pham, H. Ding, N. Sobh, M. Do, S. Patel, and G. Popescu, "Off-axis quantitative phase imaging processing using CUDA: toward real-time applications," Biomed. Opt. Express **2**(7), 1781–1793 (2011).
28. V. Mico, Z. Zalevsky, and J. García, "Common-path phase-shifting digital holographic microscopy: A way to quantitative phase imaging and superresolution," Opt. Commun. **281**(17), 4273–4281 (2008).

1. Introduction

Nowadays, there is a great variety of techniques to obtain n-phase shifts in one shot, and most of them use diffractive elements [1–4], holographic ones [5,6] or pixelated phase masks attached to a CCD camera [7], among others, to generate from 4 to 9 interferograms simultaneously [8–10]; nevertheless, some of the components utilized in these arrangements are still expensive. In order to reduce the cost of operation, we developed an alternative system that does not use diffractive elements. The proposed system is based on obtaining replicas of the shearogram using a nonpolarizing beam splitter (NPBS). We know that a polarizing phase shifting Cyclic Shear Interferometer (CSI) can generate a shearogram with circular polarization of opposite rotations after passing a quarter wave plate (QWP); if we use this shearogram as an input in a polarizing device (See Fig. 1), the device will not only create a replica of the interference pattern, it also generates a relative phase shift [1]. In this way, one interferogram is transmitted and the other one is reflected; as a result, we obtain two interference patterns with relative shifts of $\pi/2$. It is known that in lateral shearing interferometry, two mutually displaced versions of the same wavefront are able to interfere. The resulting interference pattern consists of fringes of equal wavefront slope with respect to the shear (shearograms); this allows us to directly obtain the directional derivative of the wavefront, which can be lateral or radial depending on the application. Typically a piezoelectric translator is used for phase shifting interferometry and the errors generated by this component are well-known [11,12], the technique presents the advantage of being free of non-linear phase shifting unlike the piezoelectric-depending ones [12–14]; another advantage is that the system is immune to vibrations because the reference wavefront and the object wavefront are on a common path. Also, the shearing interferometer is insensitive to temperature and air vibrations, due to the fact that the diffractive elements are not used in the optical system. Errors caused by difference in amplitude or modulation, and errors generated by the diffraction orders upon the interference patterns are not present in our arrangement, as they are in other systems. In the following sections, we show the patterns generated by the system which have relative phase shifts of $\pi/2$; with this, we only use two interferograms,

#212965 - $15.00 USD Received 30 May 2014; revised 28 Jul 2014; accepted 29 Jul 2014; published 13 Aug 2014

avoiding the use of phase shifts. In order to process the optical phase, we utilized the Vargas-Quiroga method, which uses a Regularized Optical Flow (ROF) algorithm [15] that will allow us to analyze static and dynamic phase objects. As mentioned before, the principal advantages of this system, compared to others previously published [1–6], are that the system does not need a temporal phase shift to obtain the phase derivative, also we avoid the use of diffractive elements as pixilated masks or gratings, it is only necessary to collocate a polarizer at 0 and $\pi/4$ covering each interferogram at the image plane of the system [1,7,9].

2. Experimental setup

The experimental setup for dynamic phase imaging using parallel interferograms is shown in Fig. 1. It can be seen that the experimental set-up consists of a CSI and a polarizing beam splitter (utilizing a laser diode as the source, operating at $\lambda = 532$ *nm*; its polarization is arranged to be at 45° by using a half-wave plate HWP and a linear polarizer P at the exit of the source). The polarizing beam splitter, *PBS*, splits the incident beam into perpendicular and parallel polarizing components, and their separation x_0 is controlled by the lateral movement (Δx_0) of the mirror M_2. At the output of the CSI, a Quarter-Wave Plate (QWP) converts one of the two interfering beams into a right-handed circularly polarized beam and the second one into a left-handed circularly polarized beam [4]. Considering that a is the beam's transversal section, when $x_0 \leq a$, the result will be a single shearogram at the exit of the *CSI*. If the shearogram has the described polarization properties when it enters *NPBS*, this will transmit one pattern and reflect the other one; in this way, we will have two shearograms. Considering the *NPBS* and the polarizer-array (covering each one of interferograms) as a polarizing device, where the polarizer array consists of two polarizer's with their polarizations crossed at a $\pi/4$ angle to each other, and according to the polarization phase shifting principles [1–4], the two parallel interferogramns resulting have a phase shift of $\pi/2$. As a result, we were able to obtain the necessary two $\pi/2$–phase shifted interferograms in only one stage [7], as well as directly obtain the phase derivative of the wavefront. Figure 2 shows some representative results generated by the proposed system. In Fig. 2(a) we show the characteristic interferograms of spherical aberration, which are generated with a collimating lens collocated out of focus or misaligned, in the same figure, x_1 represents the adjustable separation between the two interferograms which is achieved by moving mirror M_3. Figure 2(b) shows three micro-particles fixed on a slide (enclosed in a circle). Figure 2(c) was generated using water with baking-soda (which created an effervescence effect) to obtain bubbles that ascend and create flow lines. In Fig. 2(d) are presented the parallel interferograms of a thin candle flame, it can be seen that the parallel patterns are distorted when placing the flame.

#212965 - $15.00 USD Received 30 May 2014; revised 28 Jul 2014; accepted 29 Jul 2014; published 13 Aug 2014

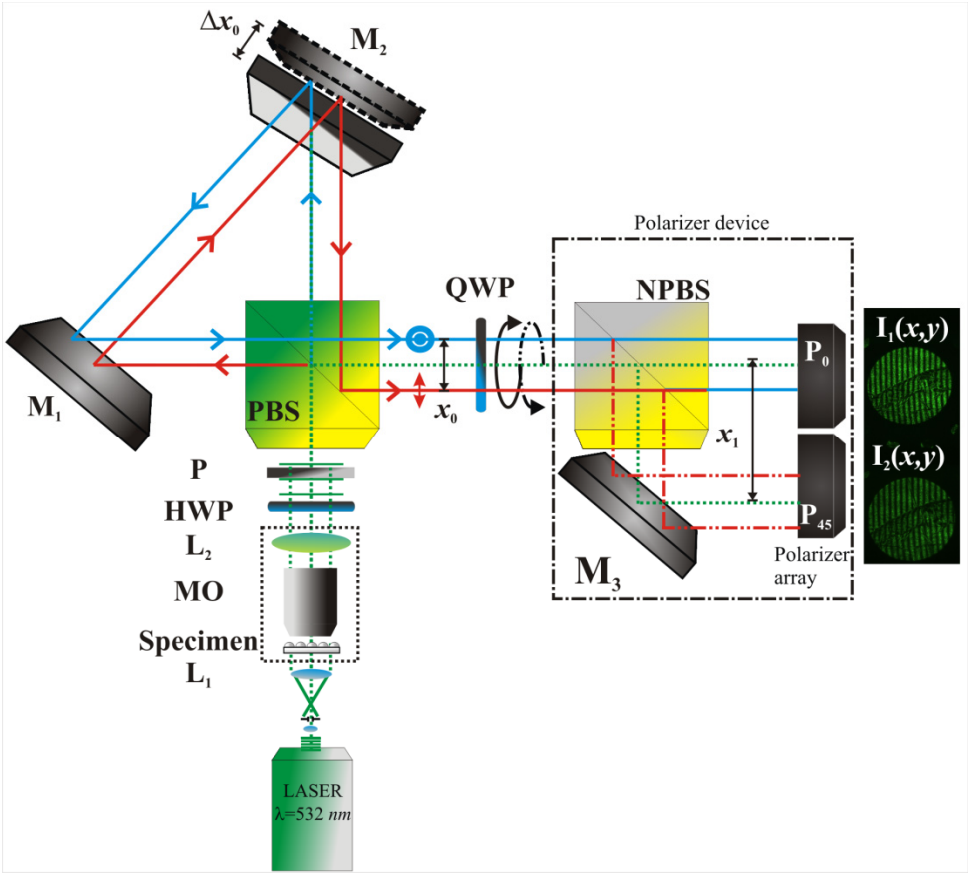

Fig. 1. Parallel phase shifting interferometry. L_i: lenses. MO: Microscope objective(40X). HWP: Half Wave Plate. P: polarizer filters. M_i: Mirrors. Δx_0: Adjustment of mirrors. x_0: beam separation. x_1: shearograms separation. PBS: polarizer beam splitter. QWP: Quarter Wave Plate. NPBS: nonpolarizer beam splitter. $I_i(x,y)$: Interference patterns.

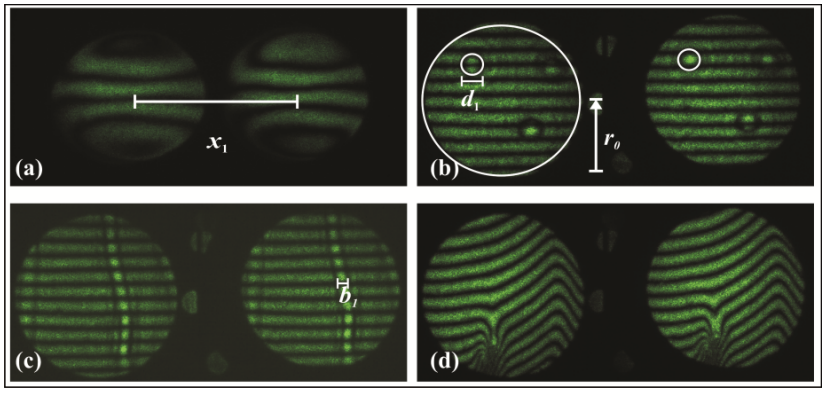

Fig. 2. Experimental results. (a) Characteristic pattern with relative phase shifts of $\pi/2$. (b) Interference patterns generated for the system with shear in the y direction; the circle shows one of 3 microparticles of diameter $d_1 \approx 0.5\,mm$. (c) Parallel representative patterns of a phase fluid ($d_1 \approx 0.5\,mm$). (d) Parallel representative patterns of dynamic phase induced by the change of refraction index induced by a candle flame. $r_0 \approx 2\,mm$.

#212965 - $15.00 USD Received 30 May 2014; revised 28 Jul 2014; accepted 29 Jul 2014; published 13 Aug 2014

2.1. Two step-algorithm

The relative phase is calculated by means of the Vargas-Quiroga method [15], which requires a constant phase shift between the interferograms that can vary between the values of 0 to 2π; the algorithm does not require the value of the shift due to the configuration of the proposed system. The two interference patterns captured by the CCD camera with a relative π/2 phase shift between them are represented as:

$$I_1(x,y) = A_0 + A_1 \sin\left[\frac{\partial\phi(x,y)}{\partial y}\right] \quad , \quad I_2(x,y) = A_0 + A_1 \cos\left[\frac{\partial\phi(x,y)}{\partial y}\right], \qquad (1)$$

where A_0 represents background illumination, A_1 is the amplitude modulation term, and $\partial\phi(x,y)/\partial y$ is the term of the phase derivative. In general, by controlling adequately the conditions of the experiment with the illumination and the angles of the retarder plates and the polarizing filters, the terms A_0 for both interferograms must be equal. The amplitude modulation terms (A_1) remain constant in both interferograms because we are not using diffractive elements to obtain the replicas, nevertheless, we apply a normalization process to the fringe patterns in order to avoid possible errors introduced by small variations of the amplitude A_0 and the modulation A_1 in both interferograms [16–19]. The algorithm that was utilized allows us to obtain the wrapped phase using both interferograms: it first obtains the direction of the fringes using a regularized optical flow method to obtain the sign of the phase; then, it applies a spiral phase transform to calculate the optical phase. Our system, along with this method, allows us to perform the analysis of static and dynamic samples. The 2π ambiguity can be retrieved by means of a phase unwrapping process, so the optical unwrapped phase can be obtained. In order to remove the background phase, the phase retrieval procedure should include a phase reference in step where the background is measured beforehand [9,10], in other words, the background phase is calculated without the target object.

We know that the phase of a shearogram is proportional to the deformation, namely, the derivative of the displacement; considering it, when an object is illuminated by a single collimated beam, the relationship between the phase difference and the change in displacement [20–23] is obtained from:

$$\frac{\partial\phi(x,y)}{\partial y} = \frac{2\pi}{\lambda}\cdot\left[\sin\theta\frac{\partial du}{\partial y} + (1+\cos\theta)\frac{\partial w}{\partial y}\right]\Delta y, \qquad (2)$$

where ***u*** and ***w*** specify the displacement components. The fringe pattern has contributions from the deformation $\partial u/\partial y$ and the slope $\partial w/\partial y$. If we consider that a phase object transmits incident light and it is illuminated in the normal direction ($\theta = 0°$). This is:

$$\frac{\partial\phi(x,y)}{\partial y} = \frac{4\pi}{\lambda}\cdot\left[\frac{\partial w(x,y)}{\partial y}\right]\Delta y_0. \qquad (3)$$

where Δy_0 is the introduced lateral shear. The phase difference provides the partial derivative of the out-of-plane displacement for this case the slope only [24]. In this case, if we want to obtain the phase, we have to integrate the slope in both directions; nevertheless, in this stage of the work we present the measurement of the slope since it gives us the information of the variations of the object in the shear's direction [16].

3. Dynamic and static experimental results

The parallel interferograms were acquired by a 3.0 Megapixel CMOS sensor (color camera) with 2048 × 1536 pixels (pixel size, 3.2 x 3.2 μ*m*). The laser beam is expanded to a diameter

#212965 - $15.00 USD Received 30 May 2014; revised 28 Jul 2014; accepted 29 Jul 2014; published 13 Aug 2014

of 10 mm, the microscope objective used has a magnification $M = 40$ and numerical aperture NA = 0.6. The CCD camera is adjusted to capture the images of two interference patterns simultaneously; each pattern was filtered using a conventional low-pass filter to remove sharp edges and details. One of the advantages of the system is that diffractive elements are not included to generate the two patterns. Consequently, it is not necessary to make corrections in fringe modulation. Figure 3 shows the experimental results obtained after placing microparticles (with a diameter of $d_1 \approx 0.5\ mm$) collocated over a microscope slide. In Fig. 3(a) shows the changes of the z-directions introduced by the microparticles, it modifies the surface of slide, the phase changes introduced by the microparticles would be equivalent to obtaining a slope as is shown in Fig. 3(b). Figures 4 and 5 show the experimental results obtained for transparent organic samples. The results shown in Fig. 4 correspond to the phase changes generated by a resin called *glycerinated gelatin* [25], which is used to fix organic samples to microscope's slides. As it can be seen, the resin introduces a phase change to the original pattern, the two patterns obtained in one shot are shown in Fig. 4(a), and its distribution is not homogeneous due to the non-uniformity of the surface, these variations are observed in the slope associated with the changes of the phase; see Fig. 4(b).

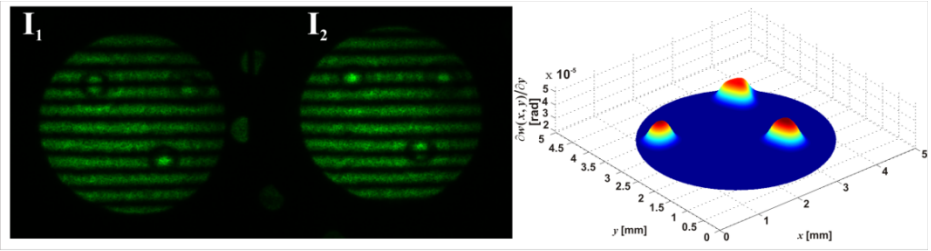

Fig. 3. Inorganic Samples. Experimental results of microparticles. (a) Parallel shearograms captured in single shot. (b) Slope.

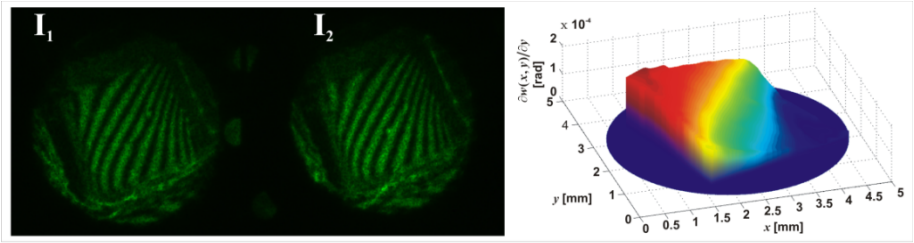

Fig. 4. Organic samples *glycerinated gelatin* on microscope slide. (a) Parallel shearograms captured in single shot. (b) Slope.

Figure 5 shows the experimental results obtained with a microarthropod called *Collembola*, which is fixed to a microscopes slide with the resin represented in Fig. 5(a), in this case, the phase changes generated for the organic sample can be clearly seen in the parallel shearograms, in Fig. 5(b) as see the slope associated with the derivative of the phase which provides indications of the associated variations with the anomalies in the morphology of the sample.

#212965 - $15.00 USD Received 30 May 2014; revised 28 Jul 2014; accepted 29 Jul 2014; published 13 Aug 2014

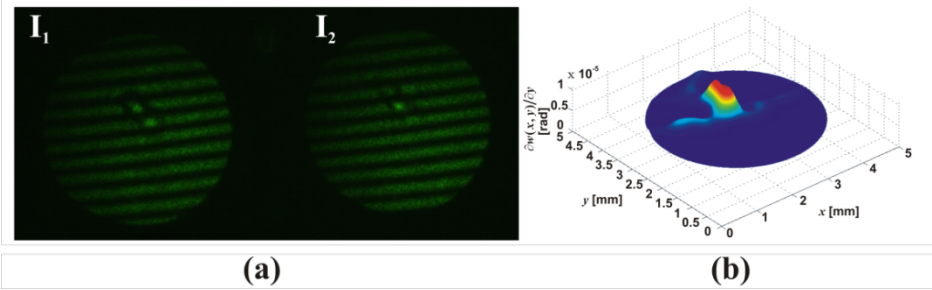

Fig. 5. Organic samples: phase change induced by the microarthropod *Collembola*. (a) Parallel shearograms captured in single shot. (b) Slope.

In order to show the advantages of the proposed system, in Fig. 6 we present the experimental results obtained with a dynamic transparent sample. Figure 6(a) shows the parallel interferograms and Fig. 6(b) presents the slope associated with the variations due to the phase. In animation (Media 1), slope associated with the phase changes generated by the flame of a candle are presented.

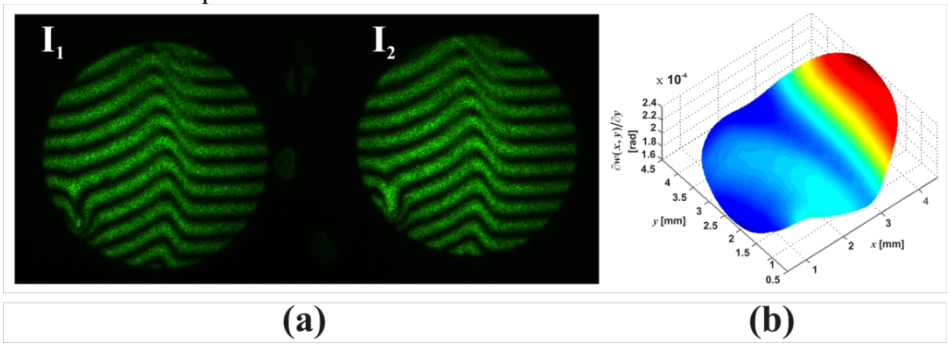

Fig. 6. Dynamic transparent sample. (a) Parallel shearograms. (b) Slope profile of a flame varying in time (Media 1).

The system can be modified to become a radial shear interferometer when a lens is placed on the trajectory of CSI, as a result, two images with slightly different in magnification will be focused at the CCD plane. Figure 7 shows the characteristic patterns of these symmetries. Figure 7(a) shows the two radial-shearograms obtained in one shot and Fig. 7(b) shows radial slope, the fringes obtained are contours of $r[\partial w(r)/\partial r]$.

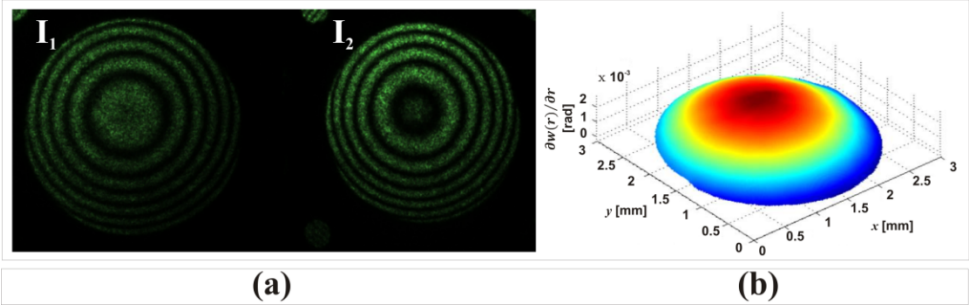

Fig. 7. Typical shearograms for radial shear obtained in a single shot. (a) Parallel shearograms of an aberrated wavefront. (b) Radial slope.

Figure 8 shows the results obtained from a sample of Red Blood Cells (RBC) collocated on a microscope slide; in this case we utilized a CSI operating in the non-shearing mode. In the results presented the sample phase is represented in terms of the optical path difference (OPD) in units of the wavelength of the utilized light source. The parallel shearograms

#212965 - $15.00 USD Received 30 May 2014; revised 28 Jul 2014; accepted 29 Jul 2014; published 13 Aug 2014

presented in Fig. 8(a) it can be clearly appreciated the RBC cells; in the animation it's observed the displacement of the sample due to gravity force (Media 2). Figures 8(b) and 8(c) present the phase reconstruction of the group of RBC, Fig. 8(d) shows the OPD for a single isolated RBC. By observing one blood cell, it can be noticed that the OPD and it allows us to calculate the mean thickness as $OPD/\Delta n = 2.28\ \mu m$ [26–28].

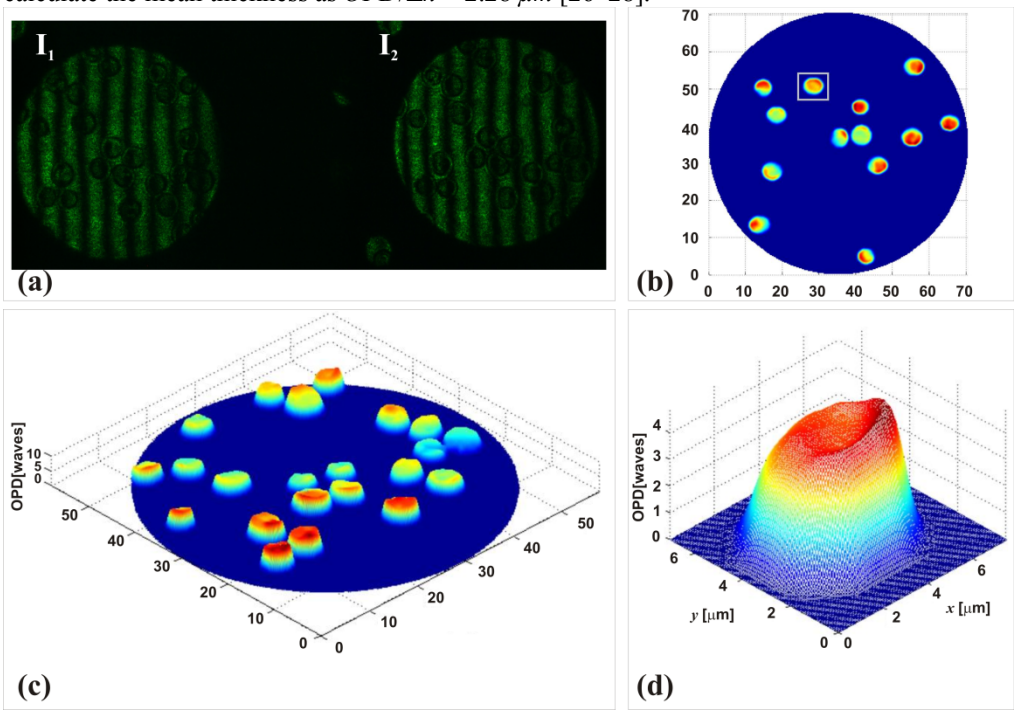

Fig. 8. Phase changes introduced by RBC smeared on a microscope slide. (a) Parallel shearograms captured in single shot (Media 2). (b)-(c) OPD. (d) Single reconstruction of RBC.

Final remarks

In this work, we proposed a new configuration for a parallel shearing interferometry system which is based on one cyclic shear interferometer that allows one to obtain the slope generated by transparent samples using two interferograms. The research provides a technique to optically obtain the first-order derivative of the phase via one shot phase-shifting interferometry. The system is considerably simpler than other proposals, use of a minimal number of optical elements, showing a suitable alternative to implement in an environment outside laboratory. In the present case, as phase shifting is achieved through polarization means, the proposed method is not suitable for birefringent transparent samples. For further applications, this system can be developed to perform parallel four-step phase shifting interferometry.

Acknowledgments

This research was supported by the Technological University of Tulancingo, according to The Initiative for the creation of the First Optics and Photonics Engineering undergraduate program in Mexico. Authors thank M. A. Ruiz for his contribution in proofreading the manuscript, comments and references from anonymous referees are also acknowledged. Author N.-I. Toto-Arellano expresses sincere appreciation to Luisa, Miguel and Damian for the support provided. Author V. H. Flores Muñoz is grateful to CONACYT for the scholarship provided (Grant. 224506).

#212965 - $15.00 USD Received 30 May 2014; revised 28 Jul 2014; accepted 29 Jul 2014; published 13 Aug 2014